

DIGITAL TWIN SIMULATION ON AXIAL COMPRESSION OF UD CFRP AND KEY PARAMETERS ON COMPRESSIVE STRENGTH

M. Ueda¹, T. Takahashi², C. Kawamura³, and T. Miyanaga⁴

¹ 1-8-14 Kanda-surugadai, Chiyoda, Tokyo, 101-8308, Japan, Nihon University

² 2-12-1 Ookayama, Meguro, Tokyo, 152-8550, Japan, Tokyo Institute of Technology

³ 3-1 Shinchu, Fuchu, Aki, Hiroshima, 730-8670, Japan, Mazda Motor Corp.

⁴ 1-13-1 Nihonbashi, Chuo, Tokyo, 103-0027, Japan, Nippon Steel Chemical & Material Co., Ltd.

Keywords: Polymer matrix composites, Carbon fiber, Compressive strength, Digital twin

ABSTRACT

The digital twin of a unidirectional carbon fiber reinforced plastic (UD CFRP) was developed using an X-ray computed tomography imaging technique. Digital twin simulation showed the scenario of compressive failure of a UD CFRP. Fiber undulation causes distributed local matrix yielding due to compressive loading. The yielded matrix lost its fiber-supporting capability, and the broadening of the matrix-yielding zone caused the lateral collapse of fibres. An analytical model to predict compressive stress-strain relation and resulting compressive strength was also presented considering the fiber undulation. The key parameters to enhance the axial compressive strength of a UD CFRP were discussed based on the analytical model.

1 INTRODUCTION

A unidirectional carbon fiber-reinforced plastic (UD CFRP) shows low longitudinal compressive strength as compared to tensile strength. A typical compression failure of a UD CFRP is fiber kinking [1-2]. It results from the instability of the fiber and matrix structure, which depends not only on the mechanical properties of the fiber, matrix, and interface but also on the composite microscopic geometry. Carbon fibers in a UD CFRP have a fiber misalignment of approximately $\pm 3^\circ$ angle at a cross-section, which influences the compressive failure [3]. X-ray computed tomography (CT) is being used to investigate the micromechanics of failures [4-5]. The technique is applied to construct a three-dimensional finite element model of a UD CFRP which replicates the actual random waviness of each fiber [6]. The simulation of compression using the three-dimensional finite element model of a UD CFRP, i.e., digital twin predicts compressive behaviour and resultant compressive strength. The numerical simulation fully reveals the fiber kinking phenomena.

In contrast, the analytical method is also important to understand the mechanics of compressive behaviour and resultant compressive strength. Based on the numerical simulation, the analytical method to predict compressive stress-strain relation is presented including prediction of the compressive strength. Key parameters to control the longitudinal compressive strength of a UD CFRP were discussed.

2 DIGITAL TWIN SIMULATION ON LONGITUDINAL AXIAL COMPRESSION

2.1 Materials and X-ray CT imaging

The materials used in this study were carbon fibers and epoxy resin. A small specimen and small compression test fixture were developed to perform a compression test of a UD CFRP in an X-ray computed tomography (CT) system. The cross-sectional images of the UD CFRP were obtained along the longitudinal direction before the compression test to develop the digital twin under intact conditions.

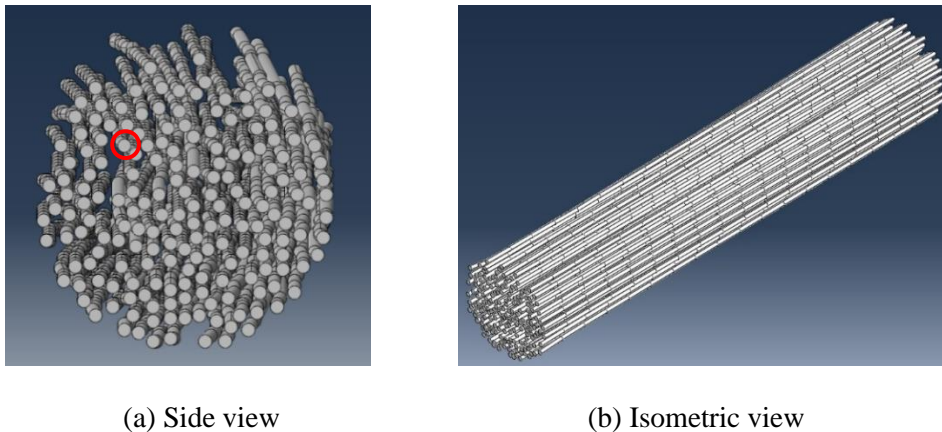
2.2 Construction of UD CFRP model based on X-ray CT images

Locations of all carbon fibers were identified in each cross-sectional CT image. Then, each fiber undulation was obtained by connecting the fiber locations along the longitudinal direction. Figure 1 shows an example of the developed fiber model. Carbon fibers align to the longitudinal direction but

have some undulation. The fiber indicated by the red circle in Figure 1(a) was extracted and shown in Figure 2. The fiber surface is not smooth because of small identification error of fiber location in the cross-sectional CT images. Since the fiber diameter is $5\mu\text{m}$, a micron-order error in the identification of fiber location causes the kinked surface. The X-ray CT image is usually blurred and causes estimation error of fiber location. Surface smoothing is possible by curve fitting of the fiber location although it was not applied. The UD CFRP model was developed based on the fiber model. The fiber model was surrounded by epoxy resin to construct the UD CFRP model as shown in Figure 3.

2.3 Numerical simulation [6,7]

Finite element simulation was performed using the developed UD CFRP model. A simple compression condition was applied to the model. The carbon fiber was supposed as elastic and epoxy resin as plastic material. Perfect bonding between the carbon fiber and epoxy resin was supposed. Finite element simulation showed that stress–strain relation was almost linear from the start of loading until reaching the maximum stress. A snapback phenomenon occurred immediately after reaching the maximum stress. Yielding in the resin occurred at various locations because the strain distribution in the resin within the UD CFRP was not uniform due to the fiber undulation. The matrix yielding started in a small zone and broadened along the fiber direction with an increase in axial compressive load. The yielded matrix does not support fibers and fibers collapse laterally. The fiber breakage accompanying kink-band formation occurs at the compression side of the bending deformation. Twisting deformations coupled with the compressive deformation during axial compression could be developed due to the fiber undulation [8].



(a) Side view (b) Isometric view
Figure 1: Fiber model developed based on the X-ray CT images.

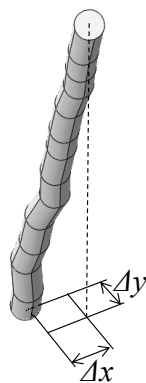


Figure 2 Extracted single fiber model.

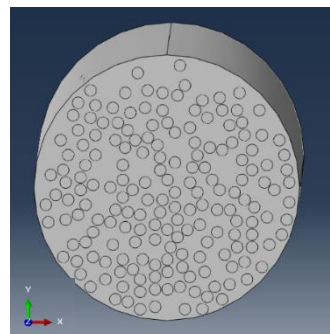


Figure 3: UD CFRP model developed based on the X-ray CT images.

The numerical simulation of the digital twin of the UD CFRP showed that the fiber undulation developed matrix yielding locally. The matrix yielding expanded with an increase of compressive loading by which the matrix lost its fiber-supporting capability causing ultimate failure. Thus, fiber undulation plays a key role in the determination of the compressive strength. In the case that exist a fiber angle clustering in a UD CFRP [9], compressive strength degraded because the matrix started to yield at the clustered zone [10].

3 ESTIMATION OF LONGITUDINAL COMPRESSIVE STRENGTH USING THE ANALYTICAL MODEL

Axial compressive stress σ_x of a UD CFRP is related to the longitudinal shear stress τ_{12} [11-12]

$$\sigma_x \approx \frac{\tau_{12}}{(\phi_0 + \gamma_{12})} \quad (1)$$

where γ_{12} is the longitudinal shear strain and ϕ_0 is the fiber misalignment angle. The maximum value of σ_x gives the axial compressive strength in the case of global fiber kinking mode. It was also shown that the axial compressive strength was the same when the local fiber kinking mode was considered [13]. However, Eq. (1) only considers a single value of fiber misalignment angle. In other words, fiber undulation is not taken into account.

Each fiber in a UD CFRP has individual undulation although all the fibers align to the longitudinal direction (the mean fiber angle is 0°). The fiber misalignment angle ϕ_0 varies within $\pm 3^\circ$ at maximum in the cross-section of a UD CFRP produced from a prepreg sheet. Thus, the fiber misalignment angle cannot be determined as a single value. The variability is often supposed to follow a normal distribution of mean fiber misalignment angle $\bar{\phi}_0$ and standard deviation Σ . The probability density function of the fiber misalignment angle is expressed as follows.

$$f(\phi_0) = \frac{1}{\sqrt{2\pi\Sigma^2}} \exp\left(-\frac{(\phi_0 - \bar{\phi}_0)^2}{2\Sigma^2}\right). \quad (2)$$

Fibers are divided into several groups based on the fiber misalignment angle to calculate the compressive load sharing. A fiber group θ_0^i is defined by fibers with the misalignment angle between ϕ_0^i and ϕ_0^{i+1} . The existing probability A^i of a fiber group θ_0^i is calculated as

$$A^i(\theta_0^i) = \int_{-\infty}^{\phi_0^{i+1}} f(\phi_0) d\phi_0 - \int_{-\infty}^{\phi_0^i} f(\phi_0) d\phi_0. \quad (3)$$

The existing probability is equal to the area ratio of the fiber group area to the whole cross-sectional area of a UD CFRP. Eq. (1) indicates that the fiber misalignment angle ϕ_0 affects the compressive behavior. Axial compressive stress is not uniform in a UD CFRP but varies depending on the local fiber misalignment angle. Thus, the axial compressive stress of a UD CFRP is obtained by summing the shared load by every fiber group as

$$\bar{\sigma}_x = \sum_i \sigma_x^i A^i \quad (4)$$

where $\sigma_x^i (= \tau_{12}/(\theta_0^i + \gamma_{12}))$ is a compressive stress of the fiber group $\theta_0^i (= (\phi_0^{i+1} + \phi_0^i)/2)$.

The in-plane shear test on an angle-ply CFRP was performed to obtain the longitudinal shear stress-strain relation. The Ramberg–Osgood equation was used to approximate the relations and shown in Figure. 4. σ_x was calculated by Eq. (1) using the Ramberg–Osgood equation.

Mean fiber misalignment angle and standard deviation were supposed as $\bar{\phi}_0 = 0$ and $\Sigma = 1.0$ following the report on prepreg-based CFRP as shown in Figure 5. The analytical compressive stress-strain curves were calculated with every 0.1° of fiber misalignment angle ($\phi_0 = \pm 0.1^\circ, \pm 0.2^\circ, \dots$) supposing uniform fiber misalignment angle. Each stress-strain curve in the case of uniform fiber misalignment angle was scaled by multiplying the area ratio to obtain the shared loads. The stress-strain curves are indicated by colored curves in Figure 6 showing each load sharing by the fiber groups with different misalignment

angles. Here, the strain recovery due to snap-through behavior was omitted because it does not happen due to load sharing by other fiber groups. The fiber group with $\phi_0=0$ carries compressive load linearly up to fiber crush stress [14-16]. Compressive loads supported by fibers are different depending on the misalignment angle. Resultant axial compressive stress is obtained by summing every shared load and shown in the bold black curve in Figure 6.

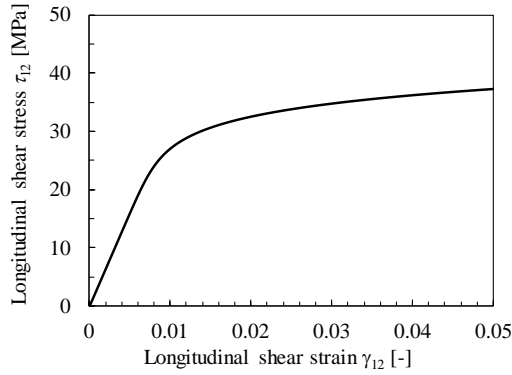


Figure 4: Longitudinal shear stress-strain relation of UD CFRP.

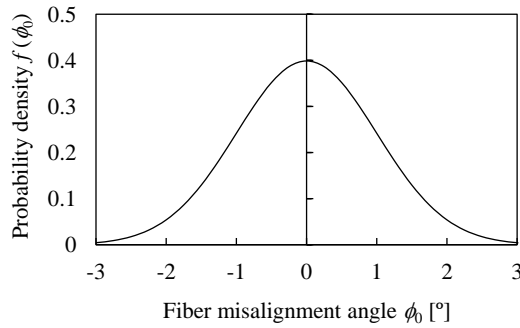


Figure 5: Probability density function of fiber misalignment angle of UD CFRP. In case of $\bar{\phi}_0=0$ and $\Sigma=1.0$.

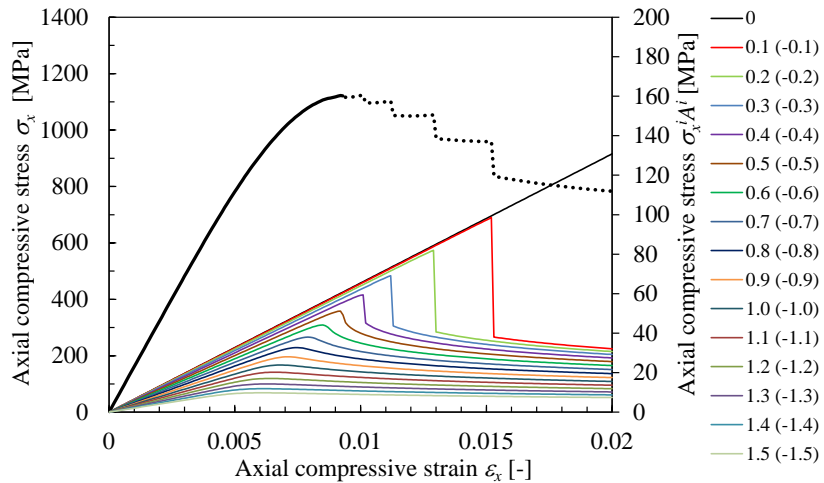


Figure 6: Analytical axial compressive stress-strain curves.

Analytical axial compressive stress-strain curve showed an almost linear increase in the initial loading. Fiber groups with large misalignment angles successively declined their load-carrying capability in descending order of the misalignment angle with an increase in compressive loading. The slope started to decrease with approaching the maximum loading. The curve became almost flat when the fiber group with the representative angle of $\theta_0^i=0.5^\circ$ reaches to the maximum point. The fiber group triggered the ultimate failure although fiber groups with misalignment angle less than 0.5° could carry more compressive load. Axial compressive strength was obtained on the assumption of zero mean fiber misalignment angle by considering the variation in the fiber misalignment angle. The fiber undulation is important to estimate the axial compressive strength.

4 KEY PARAMETERS TO ENHANCE LONGITUDINAL COMPRESSIVE STRENGTH

Key parameters to control axial compressive strength could be derived both numerically and analytically. Here, the analytical solution was selected and discussed in detail. Daniel et. al., showed a graphical interpretation of Eq. (1) as shown in Figure 7 [17]. The circled point shown in Figure 7 gives compressive strength. The point needs to raise to enhance the compressive strength. This indicates the key parameter in terms of matrix non-linear material property. Figure 7 also shows that the mean fiber misalignment angle needs to be decreased. However, it is supposed that the mean fiber misalignment angle is zero for a UD CFRP because all the fibers align to the axial direction. As shown in the previous section, variation in the fiber misalignment angle plays an important role to determine the ultimate failure. Analytical stress-strain curves indicated that compressive strength was determined by the fibers with the misalignment angle of about 0.5° due to the relatively large load drop developed by the fiber group. The standard deviation of fiber misalignment angle distribution is also a key parameter to determine compressive strength.

5 CONCLUSIONS

A three-dimensional finite element model of a continuous carbon fiber reinforced plastic was developed considering actual fiber undulation. Finite element simulation showed a compressive failure scenario. The distribution of fiber misalignment angle played an important role to trigger the ultimate failure. The axial compressive stress-strain curve was also derived analytically considering the fiber undulation. It was shown that compressive strength was obtained on the assumption of zero mean fiber misalignment angle by considering the distribution of fiber misalignment. The variation in fiber misalignment angle as well as the matrix nonlinear material property is important to determine the axial compressive strength.

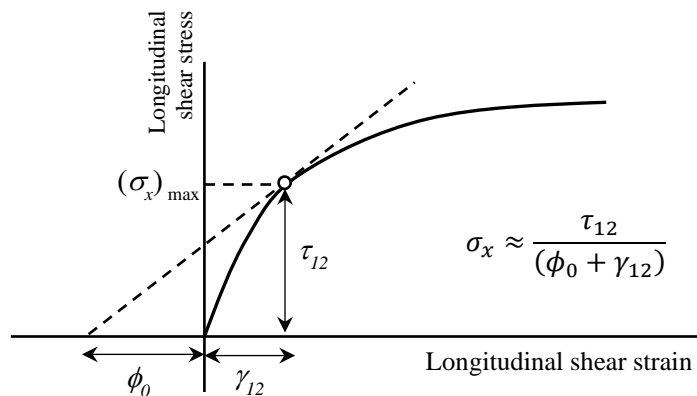


Figure 7 Longitudinal shear stress-strain relation of a UD CFRP and the determination of compressive strength: Graphical representation of Eq. (1) [17].

ACKNOWLEDGEMENTS

This work was partially supported by JSPS KAKENHI Grant Numbers 20K04184.

REFERENCES

- [1] C.R. Schultheisz, A.M. Waas, Compressive failure of composites, part I: Testing and micromechanical theories, *Progress in Aerospace Sciences*, **32**, 1996, pp. 1-42 ([doi: 10.1016/0376-0421\(94\)00002-3](https://doi.org/10.1016/0376-0421(94)00002-3)).
- [2] S. Pimenta, R. Gutkin, S.T. Pinho, P. Robinson, A micromechanical model for kink-band formation: Part I — Experimental study and numerical modelling, *Composite Science and Technology*, **69**, 2009, pp. 948-955 ([doi: 10.1016/j.compscitech.2009.02.010](https://doi.org/10.1016/j.compscitech.2009.02.010)).
- [3] T. Yokozeki, T. Ogasawara, T. Ishikawa, Nonlinear behavior and compressive strength of unidirectional and multidirectional carbon fiber composite laminates, *Composites Part A*, **37**, 2006, pp. 2069-2079 (<https://doi.org/10.1016/j.compositesa.2005.12.004>).
- [4] A.E. Scott, I. Sinclair, S.M. Spearing, M.N. Mavrogordato, W. Hepples, Influence of voids on damage mechanisms in carbon/epoxy composites determined via high resolution computed tomography, *Composite Science and Technology*, **90**, 2014, pp. 147-153 (<https://doi.org/10.1016/j.compscitech.2013.11.004>).
- [5] M. Ueda, K. Mimura, T-K Jeong, In situ observation of kink-band formation in a unidirectional carbon fiber reinforced plastic by X-ray computed tomography imaging, *Advanced Composite Materials*, **25**, 2016, pp. 31-43 (<http://dx.doi.org/10.1080/09243046.2014.973173>).
- [6] T. Takahashi, M. Ueda, K. Iizuka, A. Yoshimura, T. Yokozeki, Simulation on Kink-band formation during axial compression of a unidirectional carbon fiber reinforced plastic constructed by X-ray computed tomography images, *Advanced Composite Materials*, **28**, 2019, pp. 347-363 ([doi: 10.1080/09243046.2018.1555387](https://doi.org/10.1080/09243046.2018.1555387)).
- [7] T. Takahashi, A. Todoroki, C. Kawamura, R. Higuchi, T. Sugiyama, T. Miyanaga, K. Hattori, M. Ueda, T. Yokozeki, M. Honda, Unidirectional CFRP kinking under uniaxial compression modeled using synchrotron radiation computed tomography imaging, *Composite Structures*, **289**, 2022, 115458 ([doi: 10.1016/j.compstruct.2022.115458](https://doi.org/10.1016/j.compstruct.2022.115458)).
- [8] K. Iizuka, M. Ueda, T. Takahashi, A. Yoshimura, M. Nakayama, Development of a three-dimensional finite element model for a unidirectional carbon fiber reinforced plastic based on X-ray computed tomography images and the numerical simulation on compression, *Advanced Composite Materials*, **28**, 2019, pp. 73-85 ([doi: 10.1080/09243046.2018.1434731](https://doi.org/10.1080/09243046.2018.1434731)).
- [9] M.J. Emerson, Y. Wang, P.J. Withers, K. Conradsen, A.B. Dahl, V.A. Dahla, Quantifying fibre reorientation during axial compression of a composite through time-lapse X-ray imaging and individual fibre tracking, *Composite Science and Technology*, **168**, 2018, pp. 47-54, ([doi: 10.1016/j.compscitech.2018.08.028](https://doi.org/10.1016/j.compscitech.2018.08.028)).
- [10] T. Takahashi, M. Ueda, K. Miyoshi, A. Todoroki, Initiation and propagation of fiber kinking from fiber undulation in a unidirectional carbon fiber reinforced plastic, *Composites Part C*, **3**, 2020, 100056 (<https://doi.org/10.1016/j.jcomc.2020.100056>).
- [11] M.R. Wisnom, The effect of fibre misalignment on the compressive strength of unidirectional carbon fibre/epoxy, *Composites*, **21**, 1990, pp. 403-407 ([doi: 10.1016/0010-4361\(90\)90438-3](https://doi.org/10.1016/0010-4361(90)90438-3)).
- [12] B. Budiansky, N.A. Fleck, Compressive failure of fibre composites, *Journal of the Mechanics and Physics of Solids*, **41**, 1993, pp. 183-211 ([https://doi.org/10.1016/0022-5096\(93\)90068-Q](https://doi.org/10.1016/0022-5096(93)90068-Q)).
- [13] M. Ueda, Y. Tasaki, C. Kawamura, K. Nishida, M. Honda, K. Hattori, T. Miyanaga, T. Sugiyama, Estimation of axial compressive strength of unidirectional carbon fiber reinforced plastic considering local fiber kinking, *Composites Part C*, **6**, 2021, 100180 ([doi: 10.1016/j.jcomc.2021.100180](https://doi.org/10.1016/j.jcomc.2021.100180)).
- [14] T-K. Jeong, M. Ueda, Longitudinal compressive failure of multiple-fiber model composites for a unidirectional carbon fiber reinforced plastic, *Open Journal of Composite Materials*, **6**, 2016, pp. 8-17 ([doi: 10.4236/ojcm.2016.61002](https://doi.org/10.4236/ojcm.2016.61002)).
- [15] M. Ueda, M. Akiyama, Compression test of a single carbon fiber in a scanning electron microscope and its evaluation via finite element analysis, *Advanced Composite Materials*, **28**, 2019, pp. 57-71 (<https://doi.org/10.1080/09243046.2018.1433506>).

- [16] M. Ueda, W. Saito, R. Imahori, D. Kanazawa, T-K. Jeong, Longitudinal direct compression test of a single carbon fiber in a scanning electron microscope, *Composites Part A*, **67**, 2014, pp. 96-101 ([doi:10.1016/j.compositesa.2014.08.021](https://doi.org/10.1016/j.compositesa.2014.08.021)).
- [17] I.M. Daniel, H.-M. Hsiao, S.-C. Wooh, Failure mechanisms in thick composites under compressive loading, *Composites Part B*, **27**, 1996, pp. 543-552 ([doi: 10.1016/1359-8368\(95\)00010-0](https://doi.org/10.1016/1359-8368(95)00010-0)).